

Diagnosing longitudinal electron bunch profiles by single-shot CTR spectrometry

A window to LWFA injection dynamics

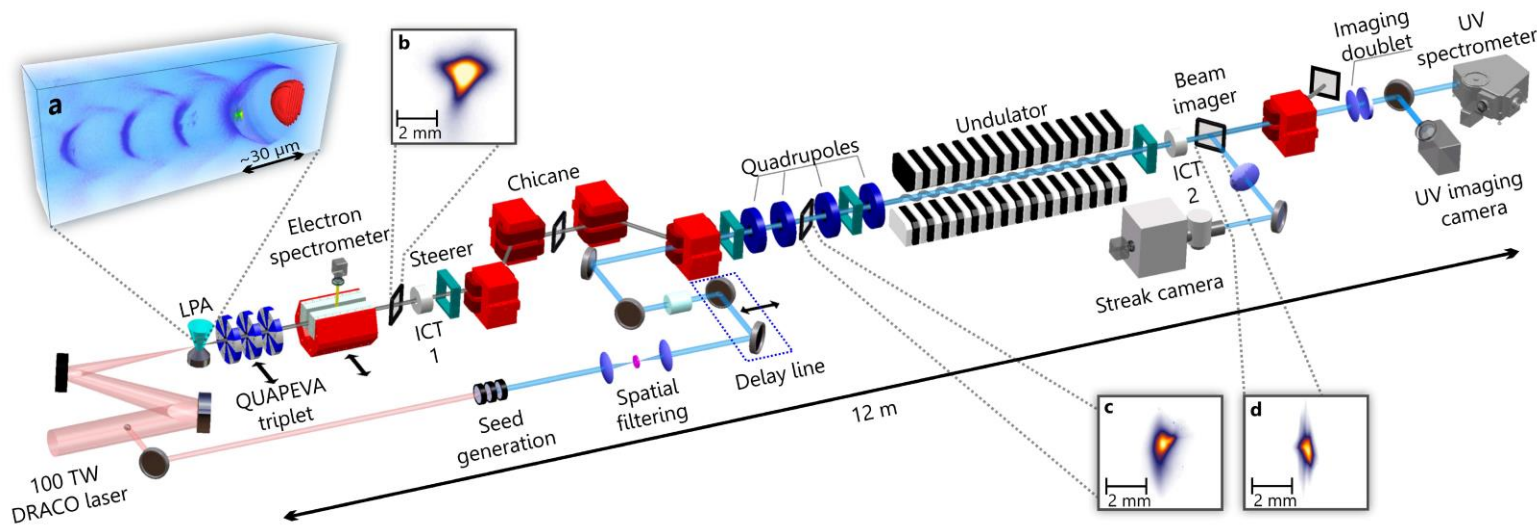
Alexander Debus¹, Omid Zarini¹, Maxwell LaBerge¹, Jurjen Couperus Cabadağ¹, Alexander Koehler¹, Thomas Kurz¹, Susanne Schoebel¹, Jessica Tiebel¹, Richard Pausch¹, Rafal Zgadzaj², Yen-Yu Chang¹, Michael Bussmann¹, Michael Downer², Arie Irman¹, Ulrich Schramm¹

¹ Helmholtz-Zentrum Dresden-Rossendorf, Dresden, Germany

² University of Texas at Austin, Austin, TX, USA

EAAC 2023, WG 7, 16:45

High brightness electron beams for future X-ray lasers



First demonstration of a seeded FEL driven by a laser plasma accelerator at HZDR

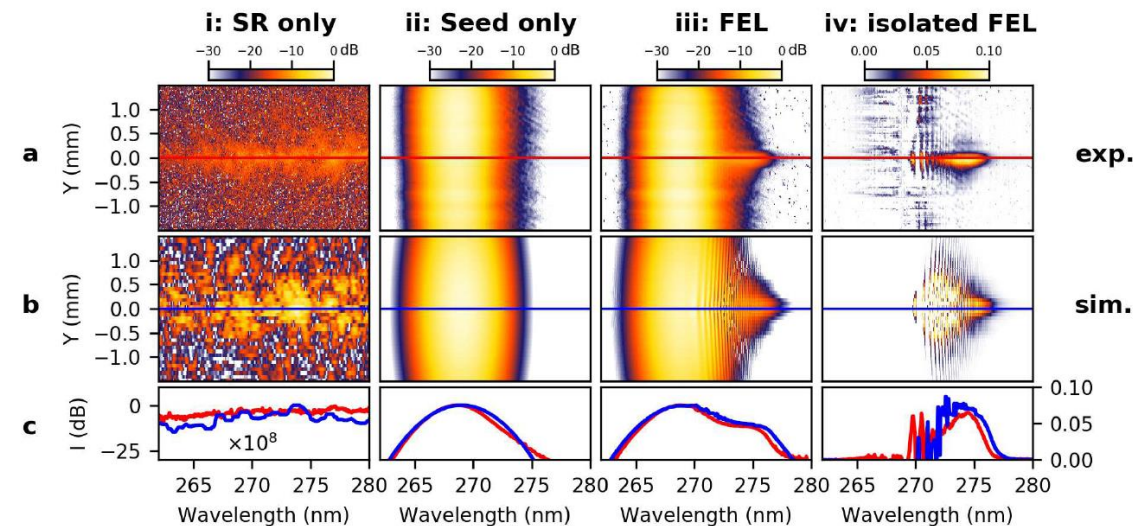
Marie Labat et al., „Seeded free-electron laser driven by a compact laser plasma accelerator“, *Nat. Photon.* (2022).

<https://doi.org/10.1038/s41566-022-01104-w>

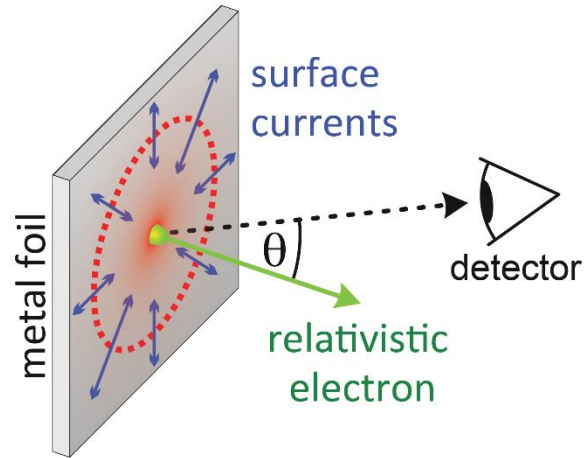
COXINEL collaboration

Motivation for measuring electron bunch profiles

- Measure, understand and control LWFA/PWFA beams.
- Micro-structures and pre-bunching are critical for designing FELs.



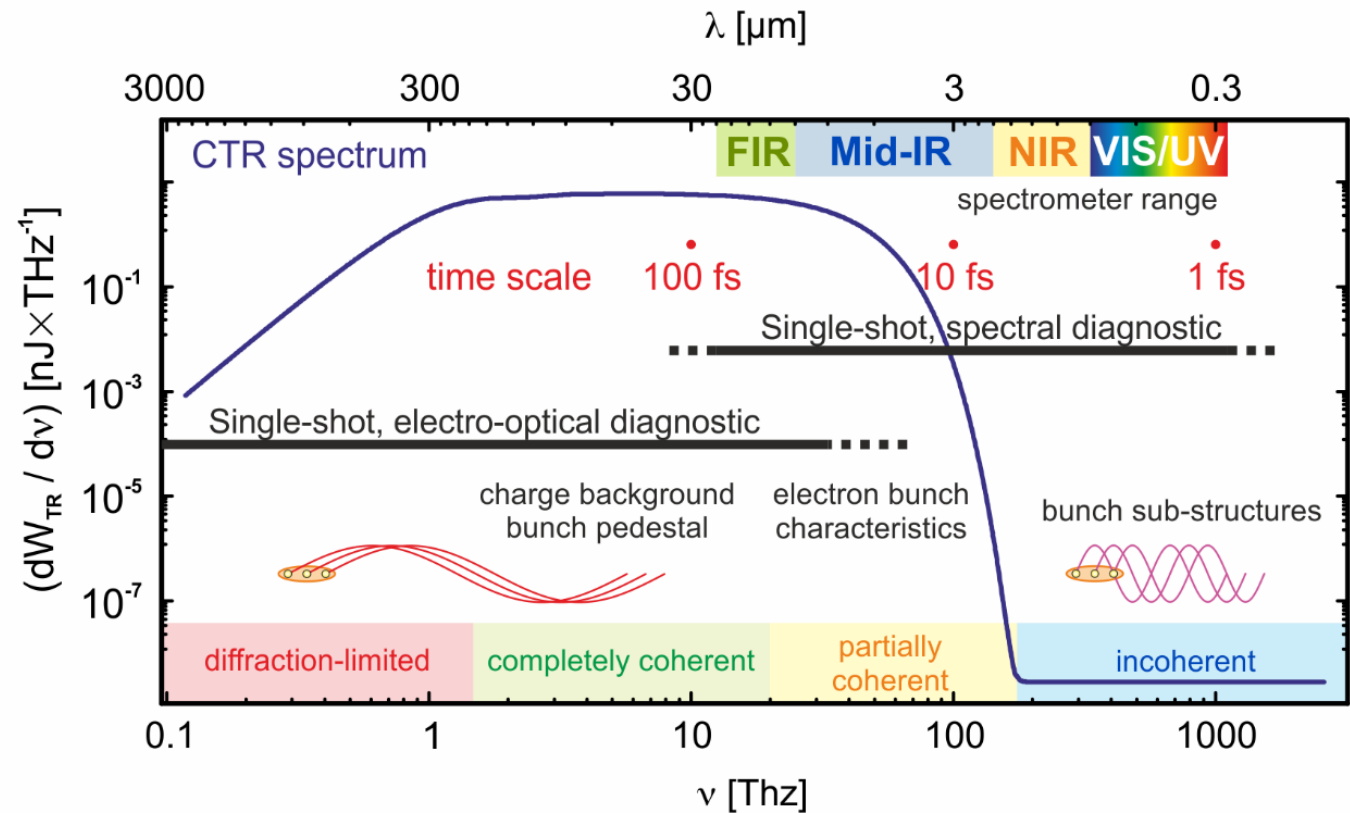
Spectral Coherent transition radiation diagnostics: A gateway to the fs-scale



$$\frac{d^2 W_e}{d\omega d\Omega} = \frac{r_e m_e c}{\pi^2} \frac{\beta^2 \sin^2 \theta}{(1 - \beta^2 \cos^2 \theta)^2}$$

- Transition radiation (TR) is emitted when a relativistic charge passes through an interface between two dielectric media.

- Broadband radiation
- Radiation directional within $1/\gamma$ -cone
- TR-beam is radially polarized



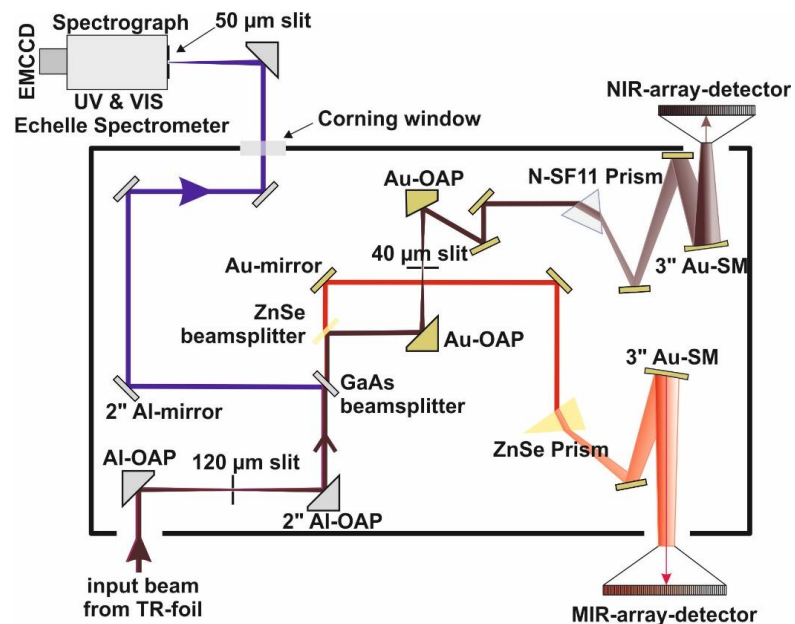
Sim: 200 MeV, 20pC, 10 fs bunch length, 20 μm diameter

Diagnostics for plasma-based electron accelerators

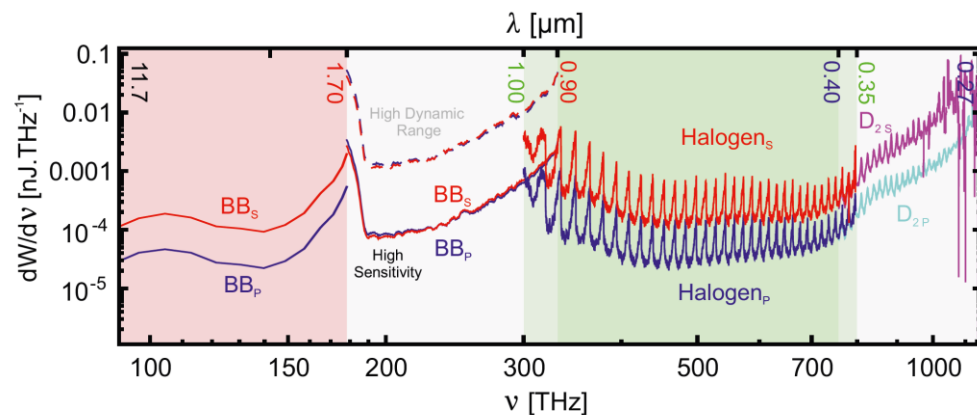
M. C. Downer, R. Zgadzaj, A. Debus, U. Schramm, and M. C. Kaluza

Rev. Mod. Phys. **90**, 035002 (2018)

Ultrabroadband UV to mid-IR spectrometer at single shot



Detection threshold curve



Omid Zarini, *et. al.*, PRAB 25, 012801, (2022)

DOI: 10.1103/PhysRevAccelBeams.25.012801

- **single-shot capability**
- 5.5 octaves frequency range
- **250 nm (UV) – 11.35 μm (MIR)**
- high spectral resolution
- high-dynamic range
- detection limit ~ 50 fJ of CTR

Wavelength calibration

Mercury-Argon lamp, Argon lamp, absorption lines of Teflon foils

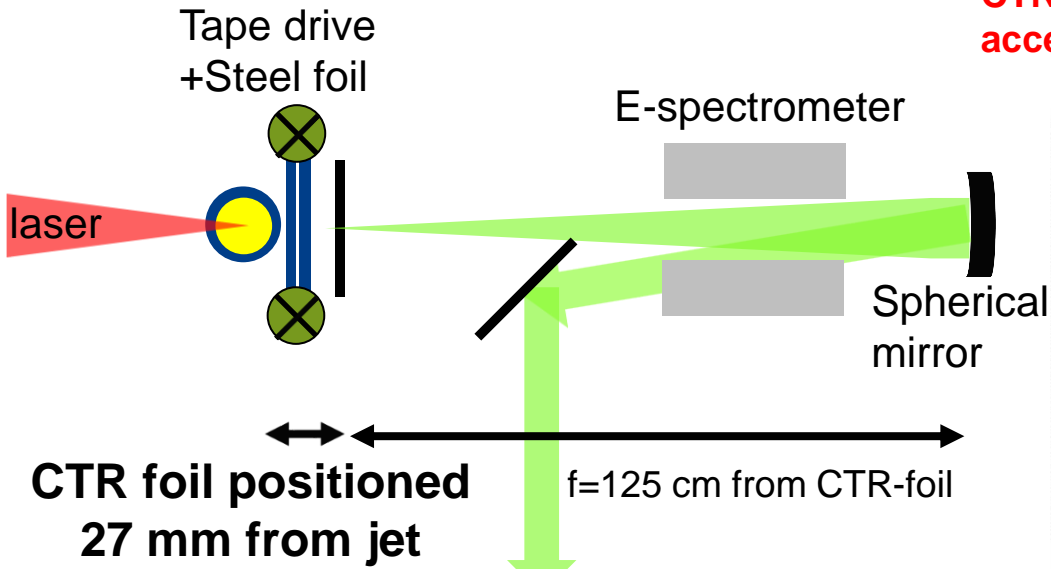
Relative response calibration

Halogen and Deuterium lamps, blackbody radiator

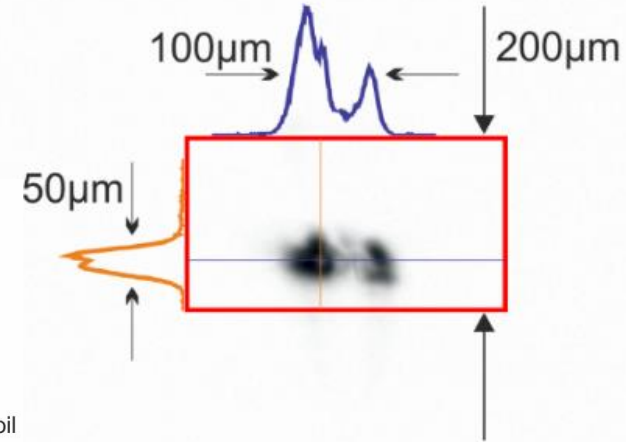
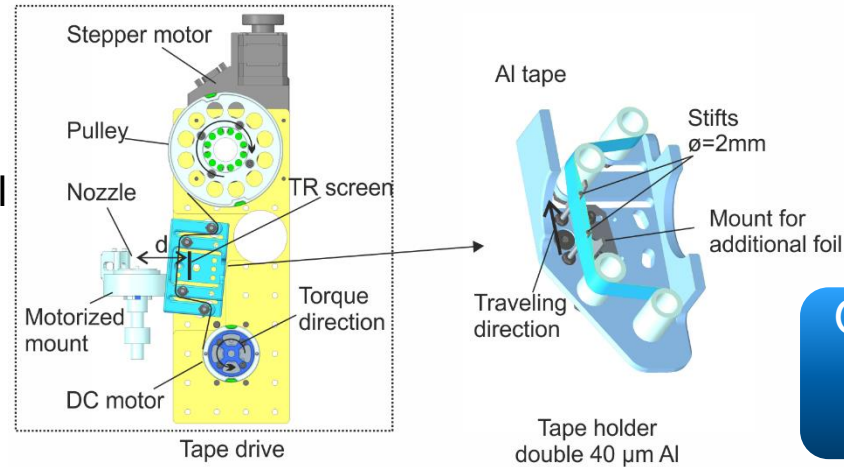
Absolute photometric calibration based on a range of laser sources

400nm, 532 nm, 800 nm, 1.5 μm and 10.6 μm

CTR foil target positioning & shielding close to source for full coherence



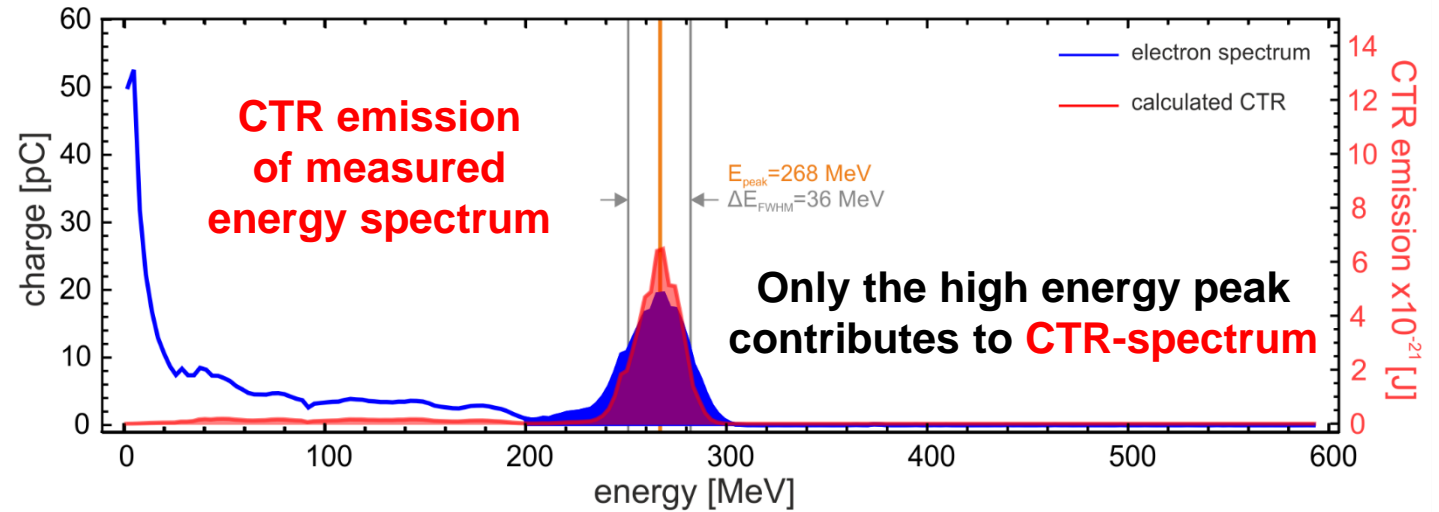
CTR-spectrometer acceptance angle $\theta \sim 16$ mrad
 $\gamma = 1/\theta \rightarrow E_{min} \sim 30$ MeV



Only select shots that make it through the CTR spectrometer aperture

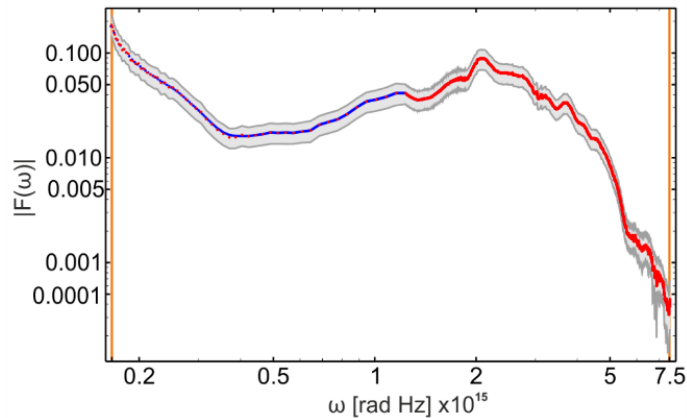
Use electron spectra with divergence information to calculate formfactor spectrum normalization of measured CTR spectrum

Exclude shots with "insufficient" electron spectra

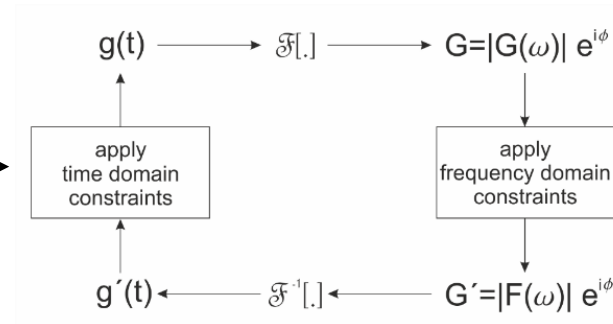


Data analysis: From the spectral to the time-domain

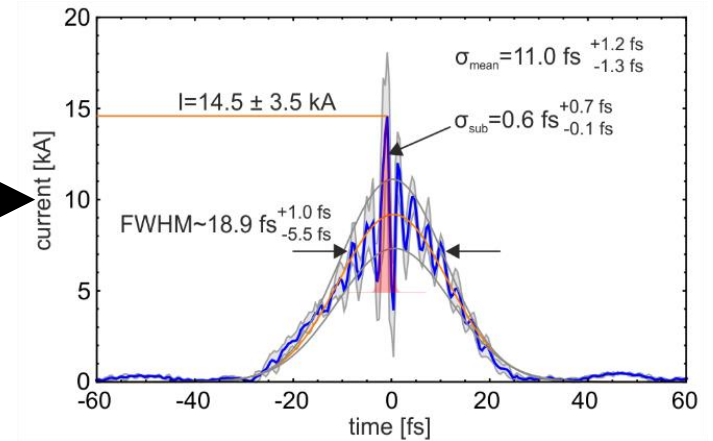
Form factor extracted from measured spectrum



Phase-retrieval including error analysis



Reconstructed electron bunch profile



Generate 50 - 150 reconstruction candidates for each shot based on variant of GS-phase retrieval algorithm

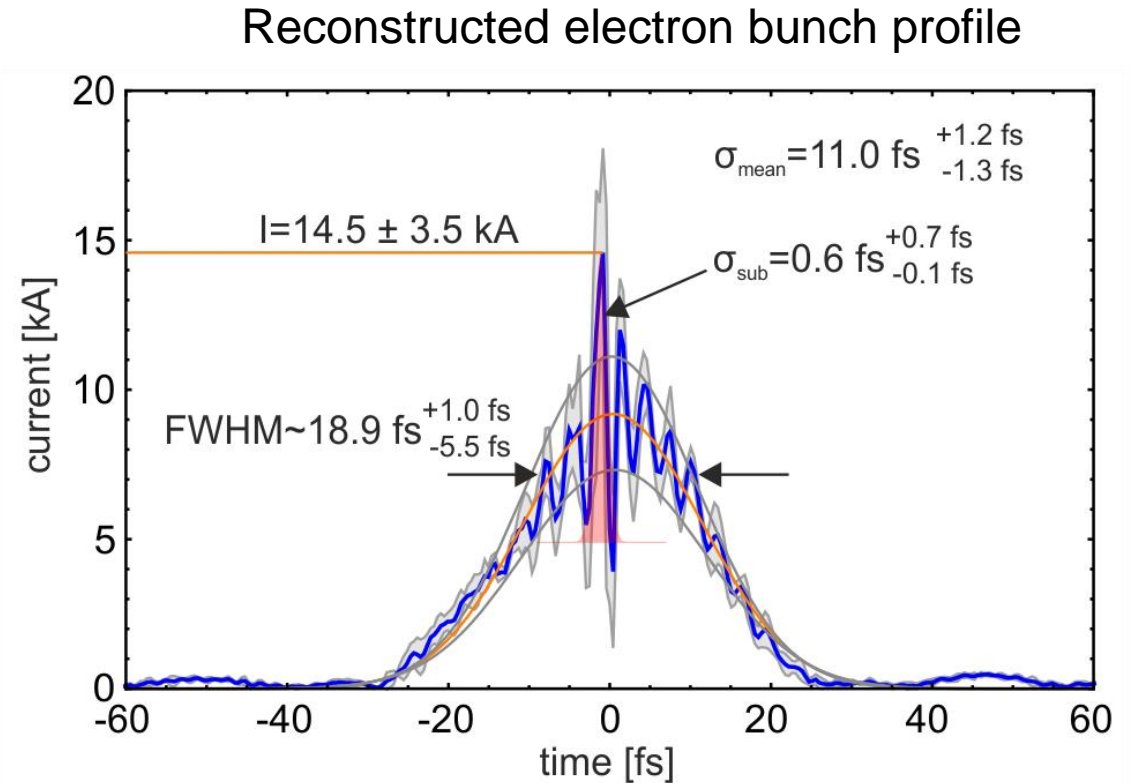
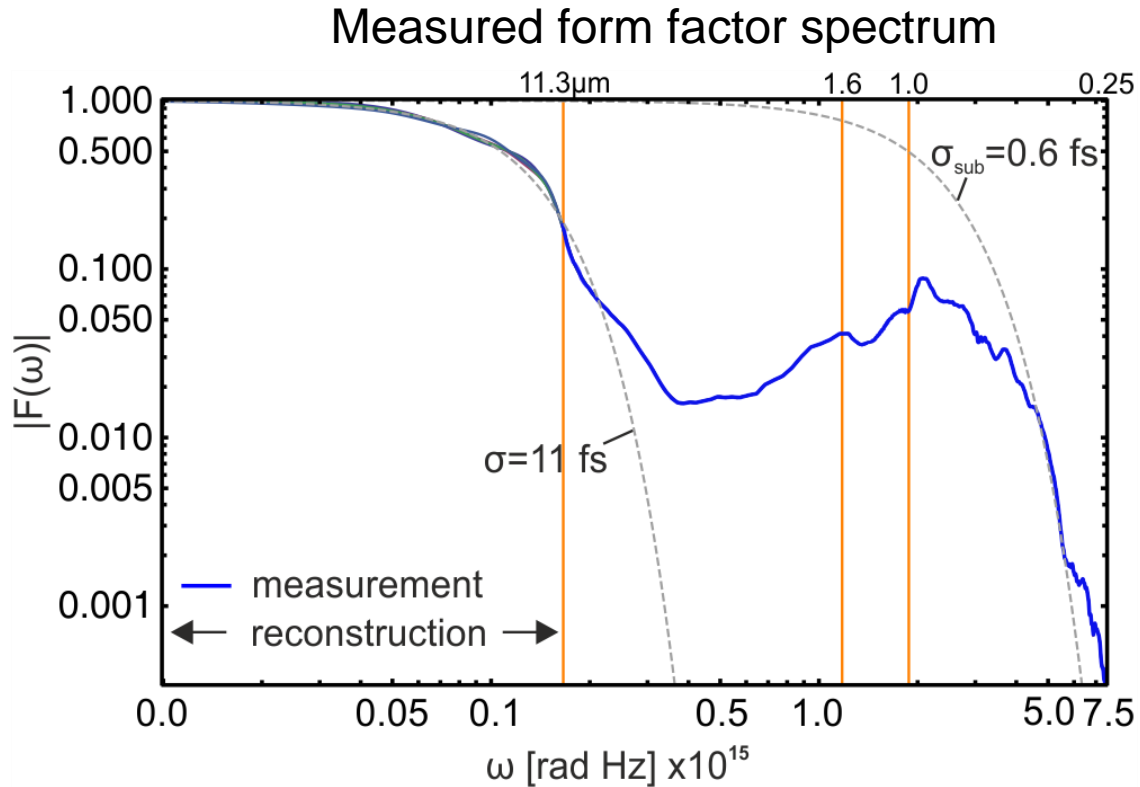
Remove reconstructions with insufficient quality-of-fit

Define metric within equivalent candidate solutions

Correlate all candidates with one another, accounting for mirror and translational ambiguity and identify differences between solution candidates (sum of diff-squared).

Apply clustering algorithm to detect ambiguous reconstruction data (multiple clusters!) and remove outliers.

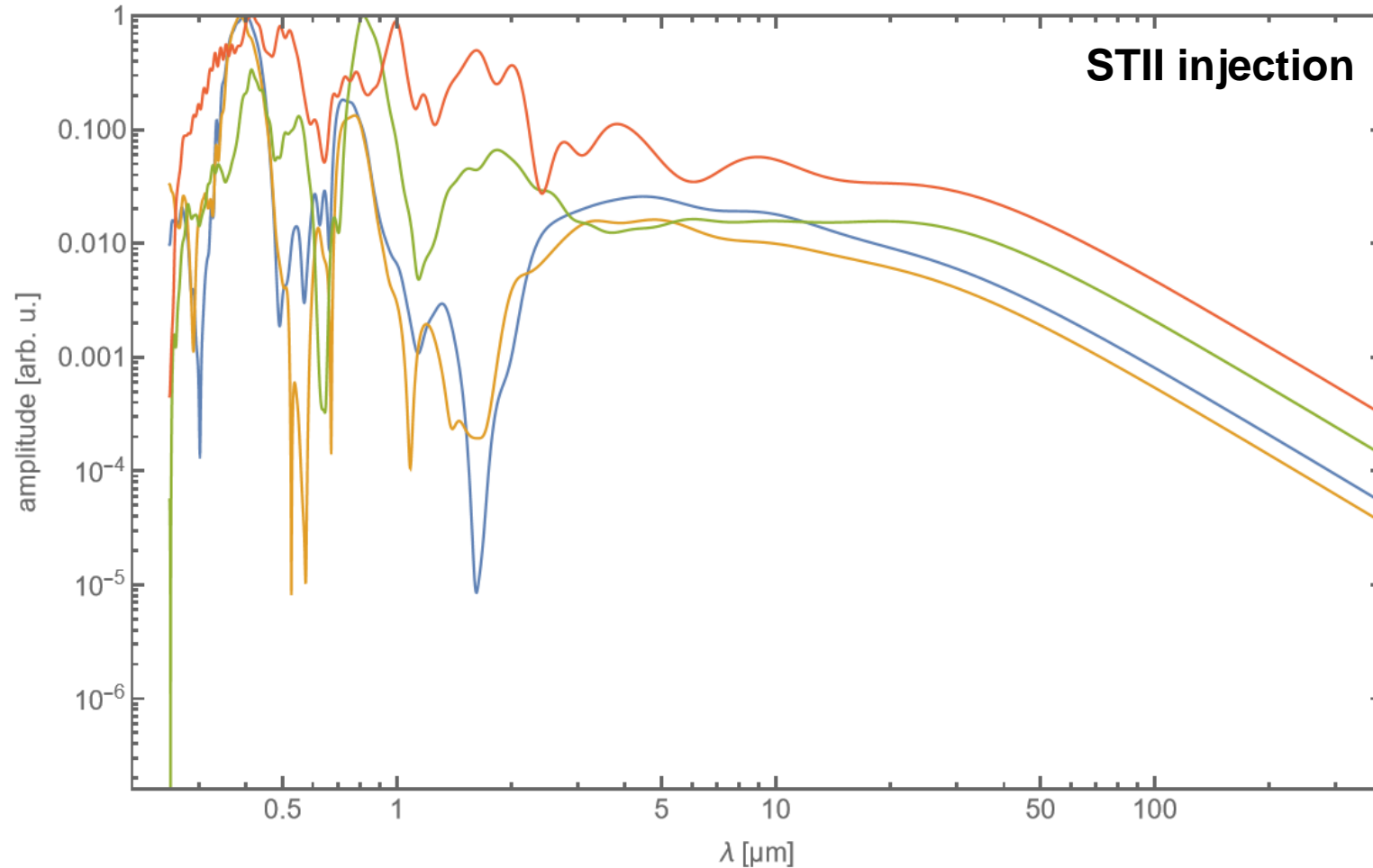
Typical electron bunch profiles extend over multiple time scales



- Bunch length: 11 fs (rms), 18.9 fs (FWHM)
- Sub-structure 0.6 fs (rms)
- Bunch within one LWFA bucket

**Typical micro-structures
are on a sub- μm scale.**

Typical micro-structures correspond to the laser wavelength scale

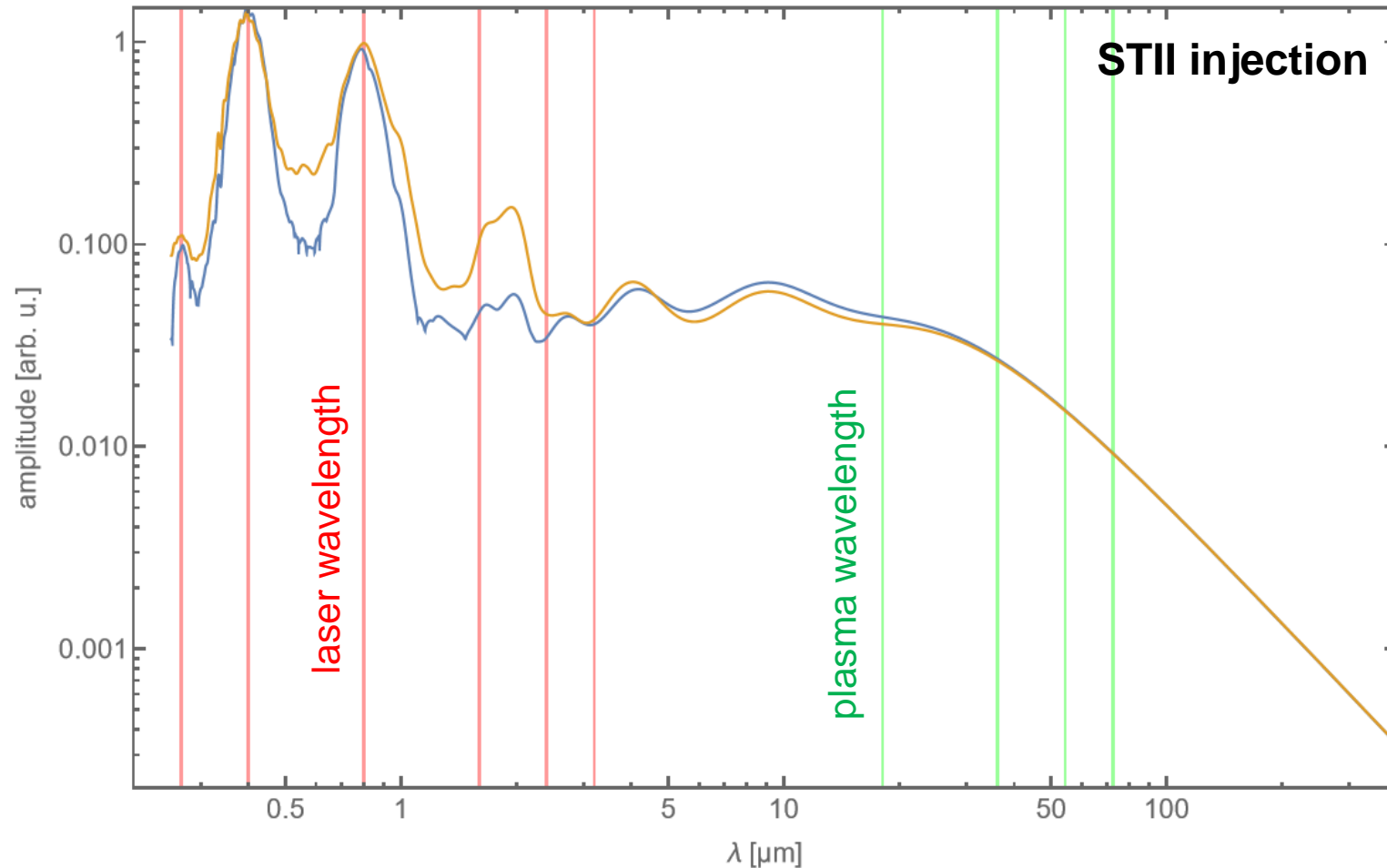


Typical formfactors magnitudes in the optical range are up to 10%.

4 randomly selected form factor spectra from an STII set at $n_e = 3.4 \cdot 10^{18} \text{ cm}^{-3}$.

Micro-structures feature significant shot-to-shot variations.

Typical micro-structures correspond to the laser wavelength scale



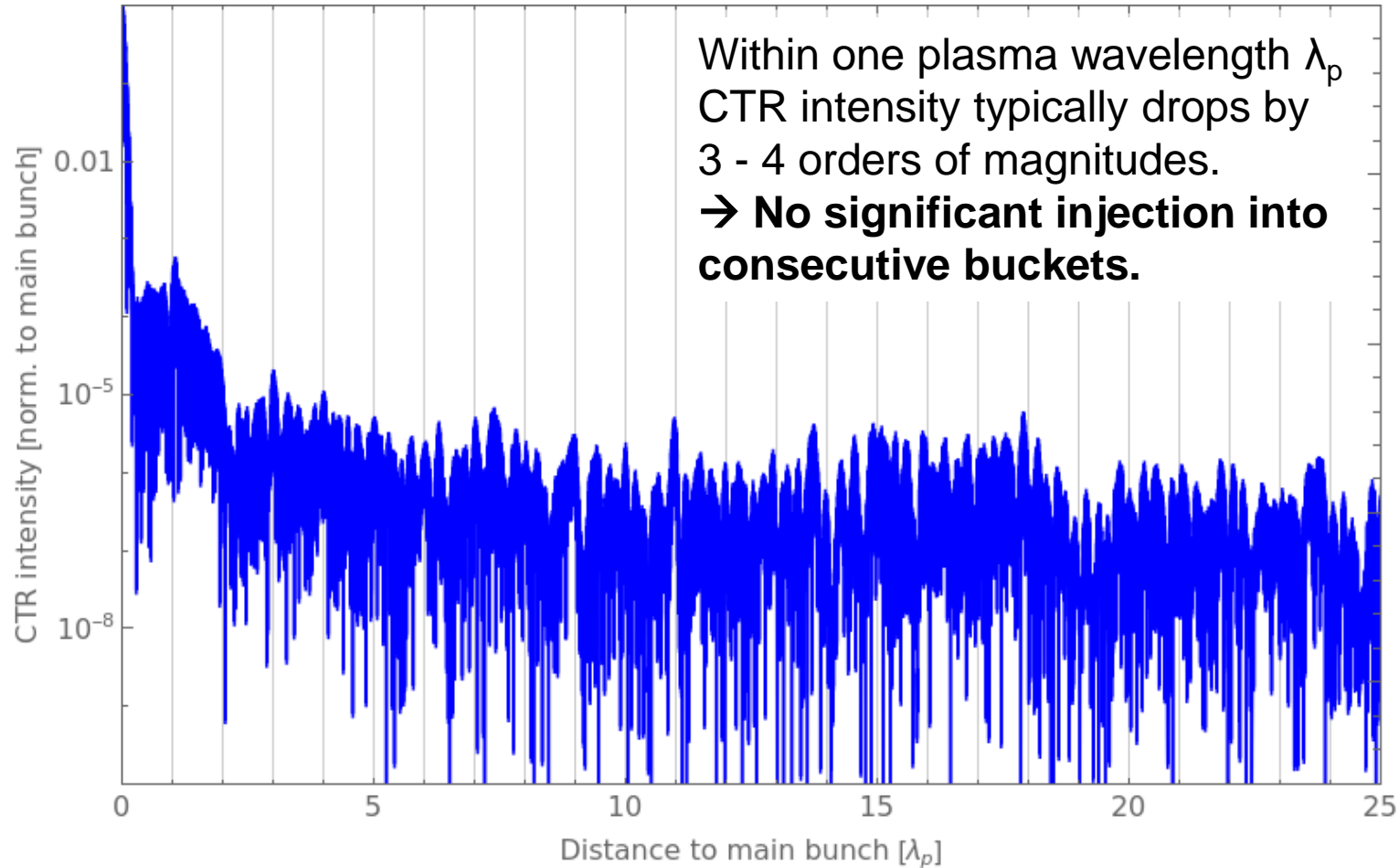
Typical formfactors magnitudes in the optical range are up to 10%.

Apply arithmetic (orange) and geometrical (blue) averages on all 58 shots of an STII set at $3.4 \cdot 10^{18} \text{ cm}^{-3}$.

Micro-structures have strong contributions from laser-electron interactions.

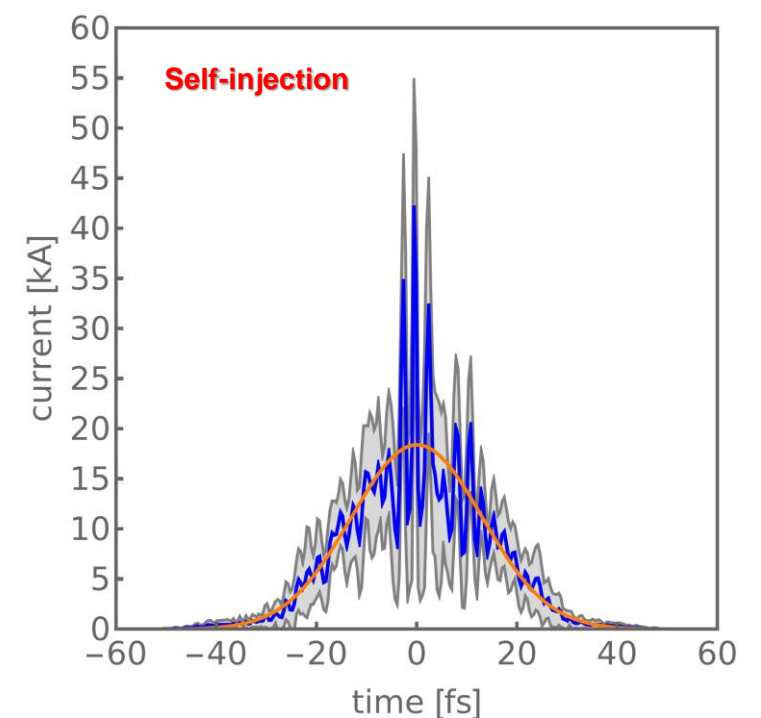
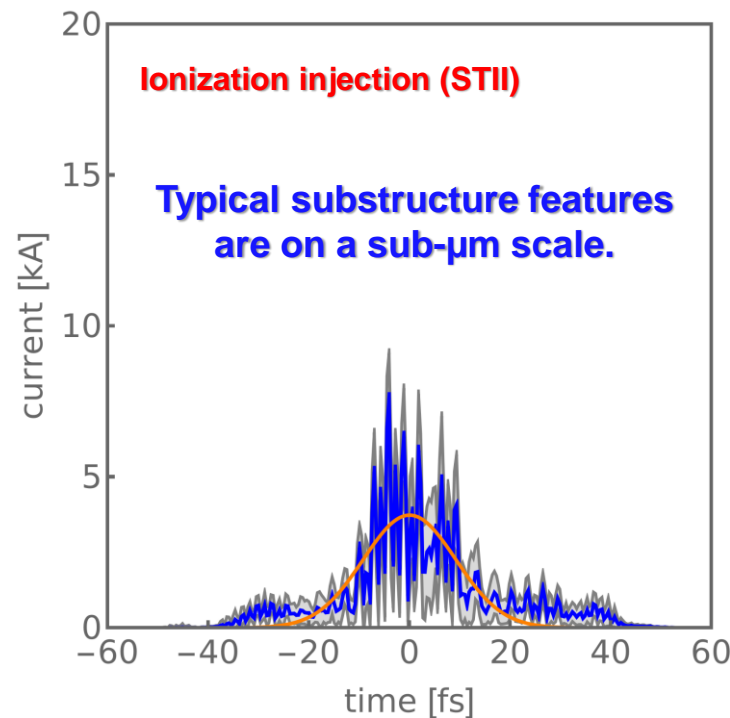
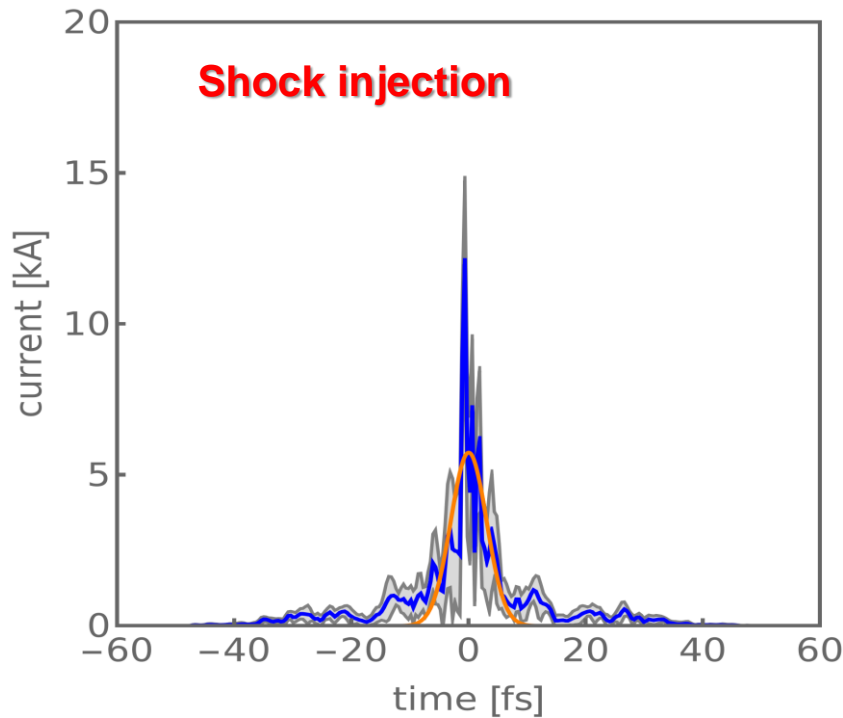
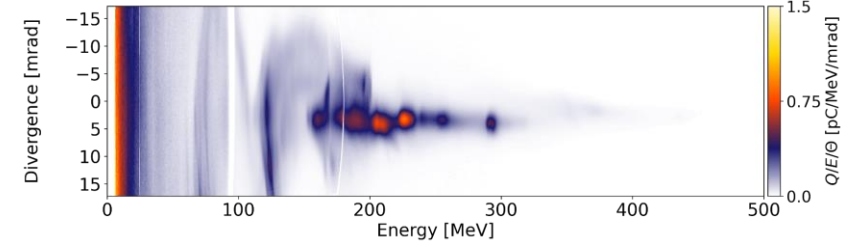
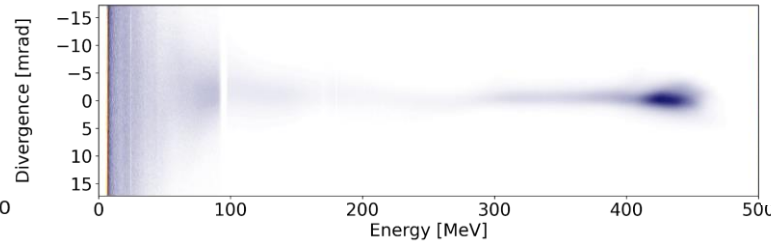
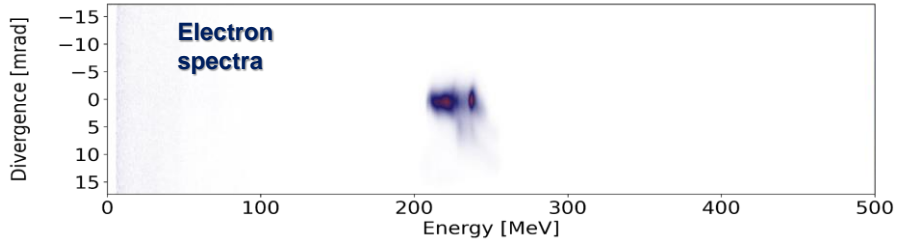
Analysis of optical CTR from Echelle spectrometer

Typically no significant injection into multiple buckets found



Analysis similar to *Lundh et al.*, Phys. Rev. Lett. 110, 065005 (2013),
„Experimental Measurements of Electron-Bunch Trains in a Laser-Plasma Accelerator”

CTR spectra quantitatively probe longitudinal LWFA injection properties

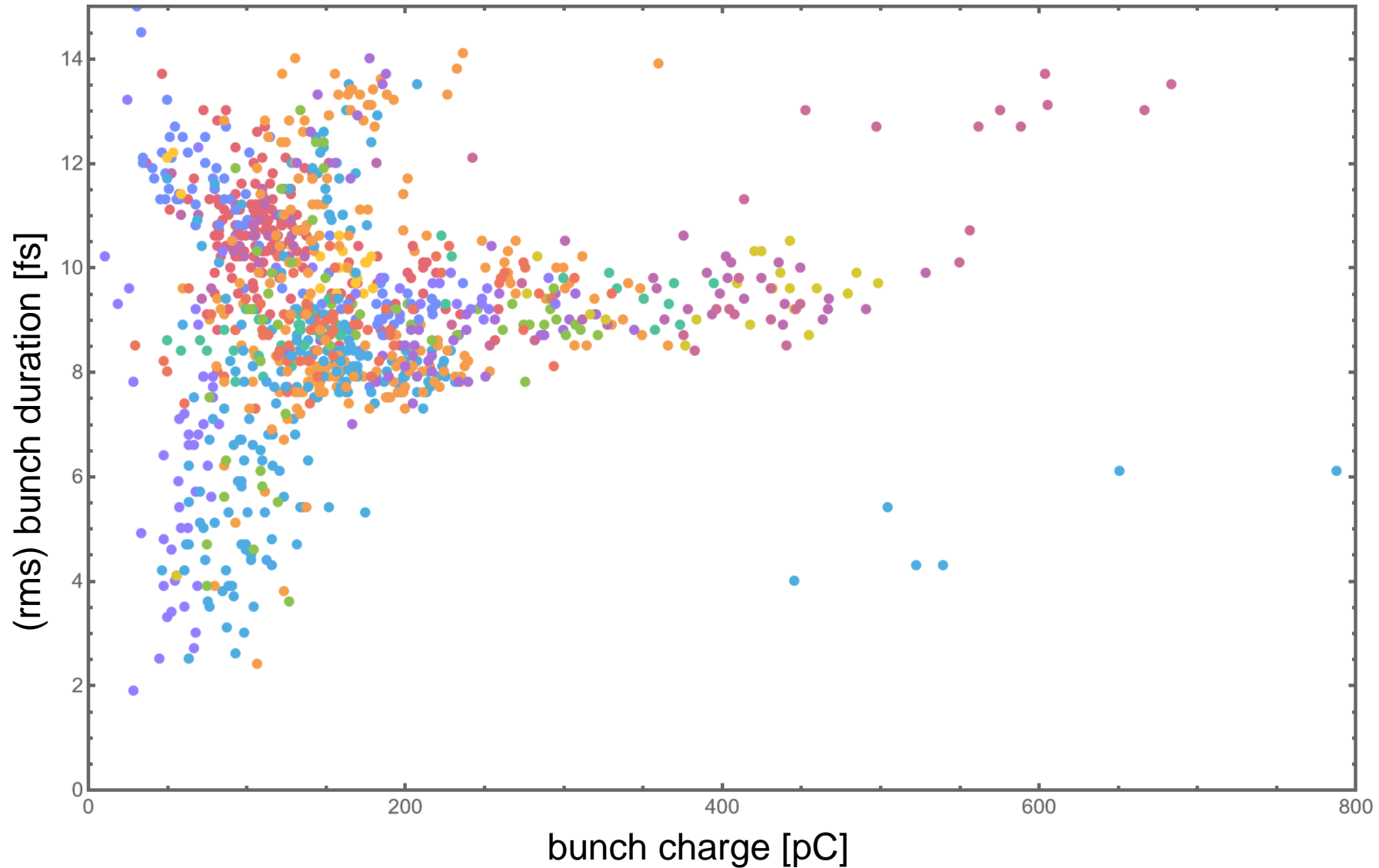


Peak charge: 68 pC (115 pC total)
FWHM-duration: 2.9 (-2.2,+0.2) fs
RMS-duration: 3.0 (-1.5,+0.6) fs
Envelope current: 5.7 (-1.2,+2.0) kA

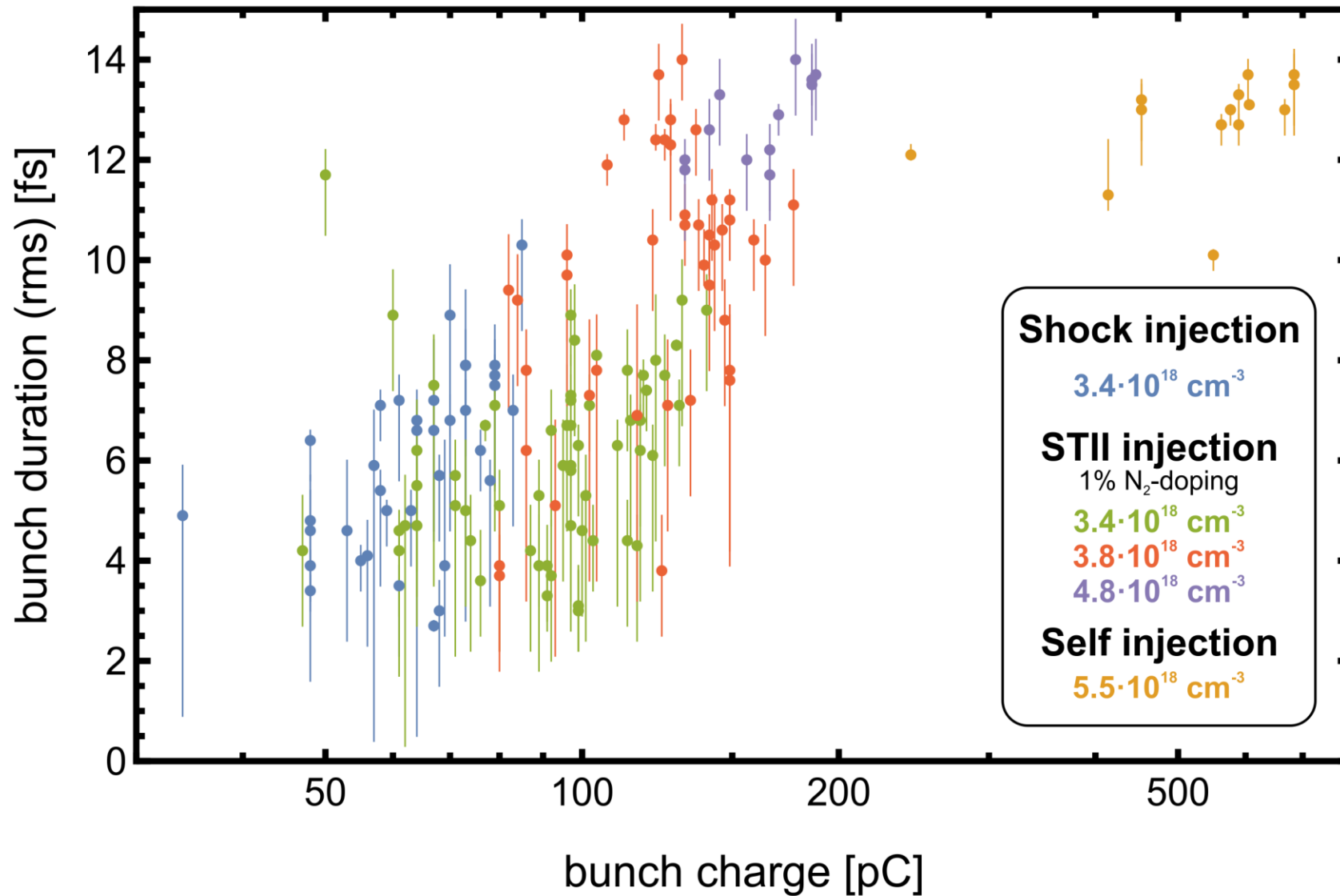
Peak charge: 102 pC (462 pC total)
FWHM-duration: 4.7 (-0.3,+1.3) fs
RMS-duration: 9.2 (-2.5,+1.2) fs
Envelope current: 3.7 (-1.4,+1.4) kA

Peak charge: 606 pC (1450 pC total)
FWHM-duration: 5.7 (-2.8,+3.1) fs
RMS-duration: 13.1 (-0.0,+0.1) fs
Envelope current: 18.4 (-8.7,+8.7) kA

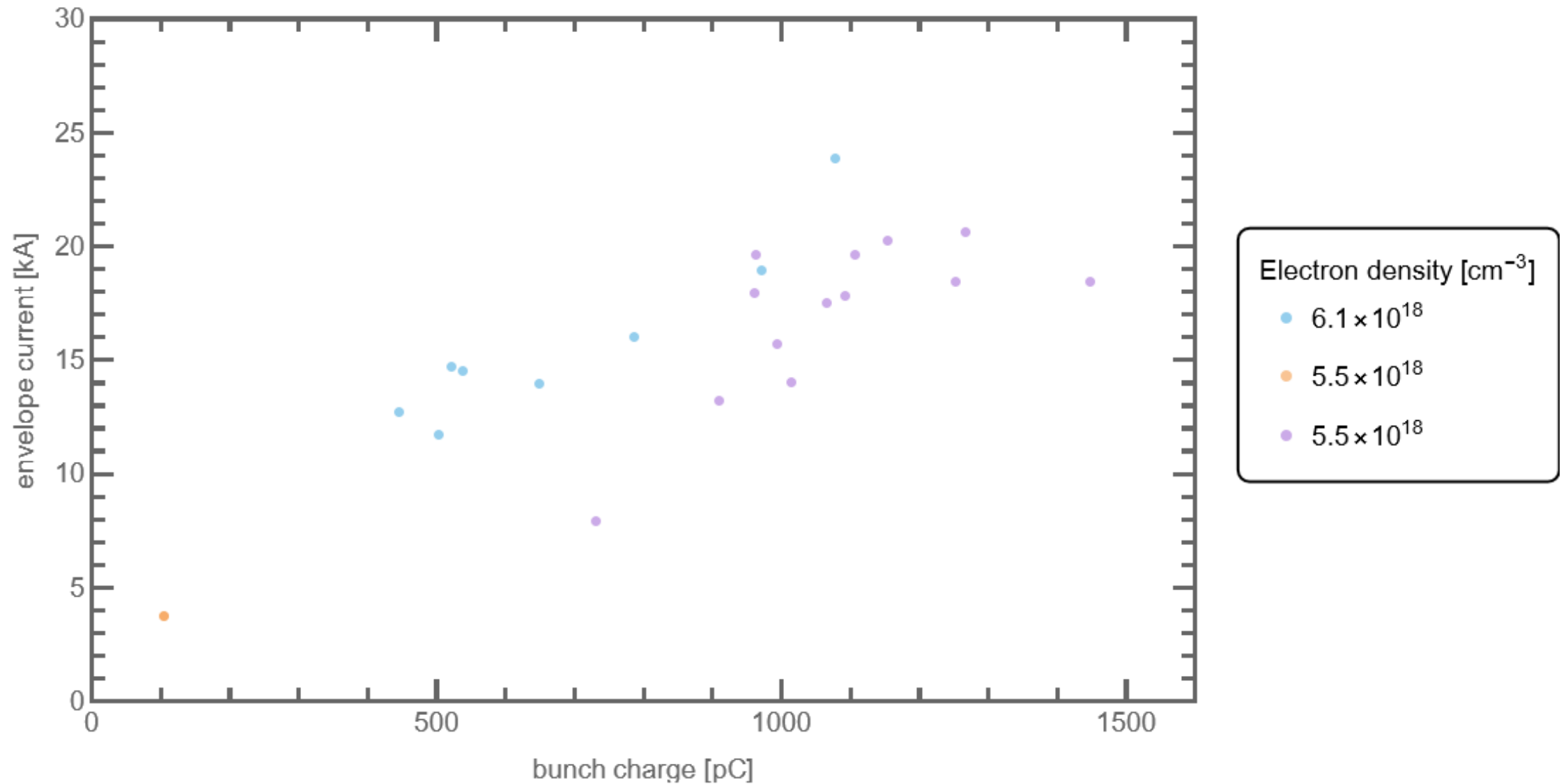
Birds-eye-view: Over 780 qualified shots for CTR analysis



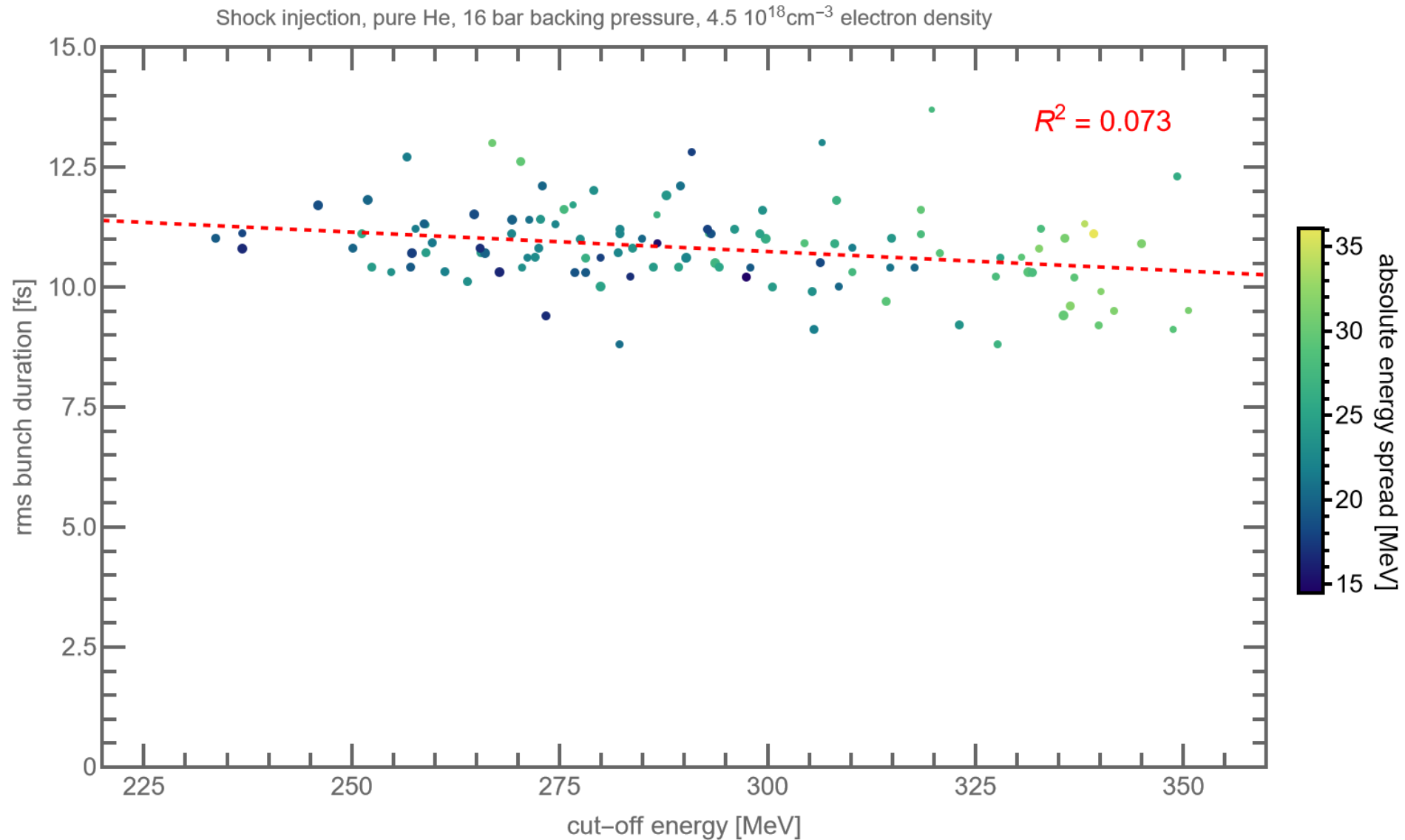
CTR spectra quantitatively probe longitudinal LWFA injection properties



As expected: Self-injection varies unpredictably from shot to shot.



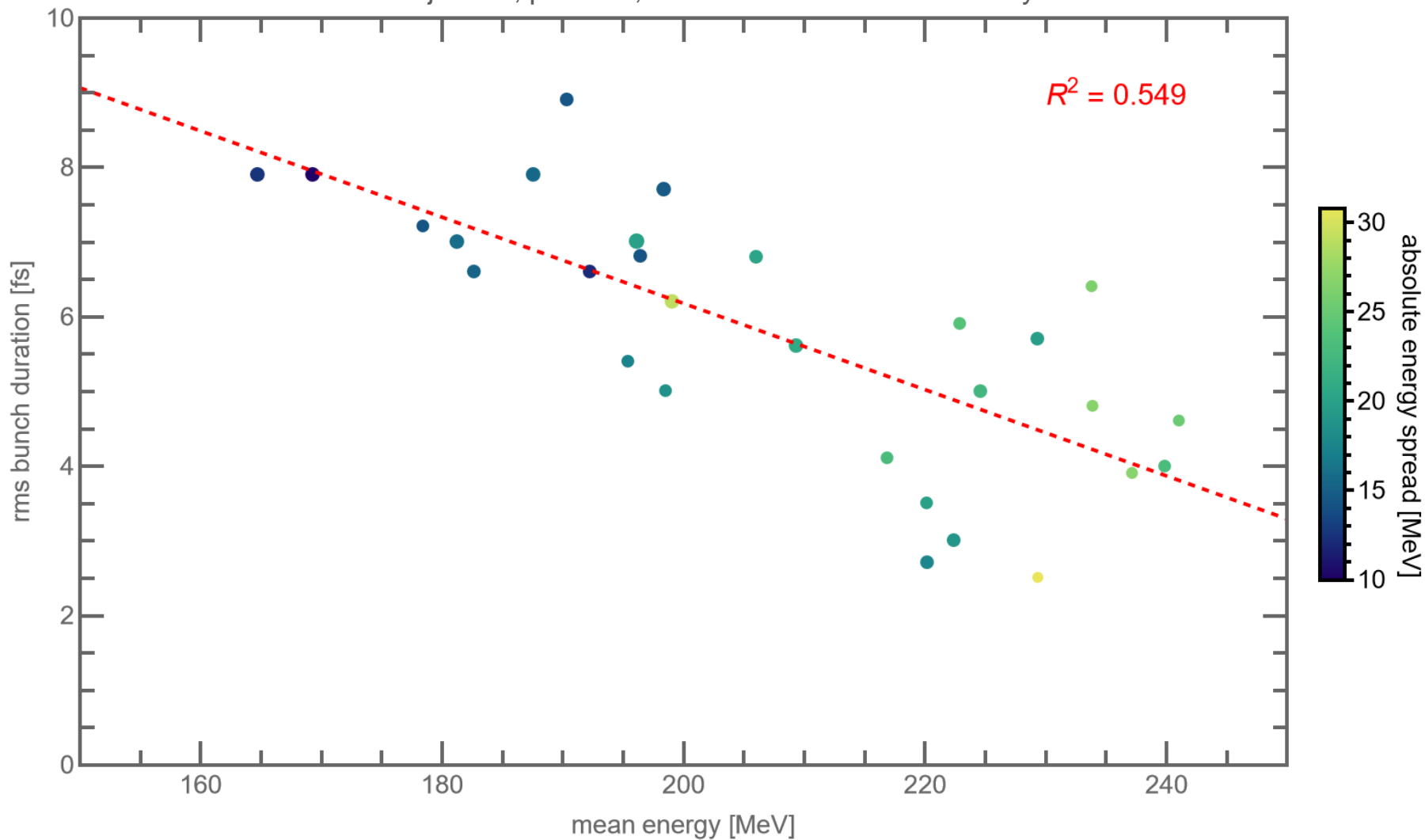
Shock and STII regimes often feature low shot-to-shot variations



Dot-areas are proportional to bunch charge.

Correlations in shock injection: Bunch duration vs. mean energy spread

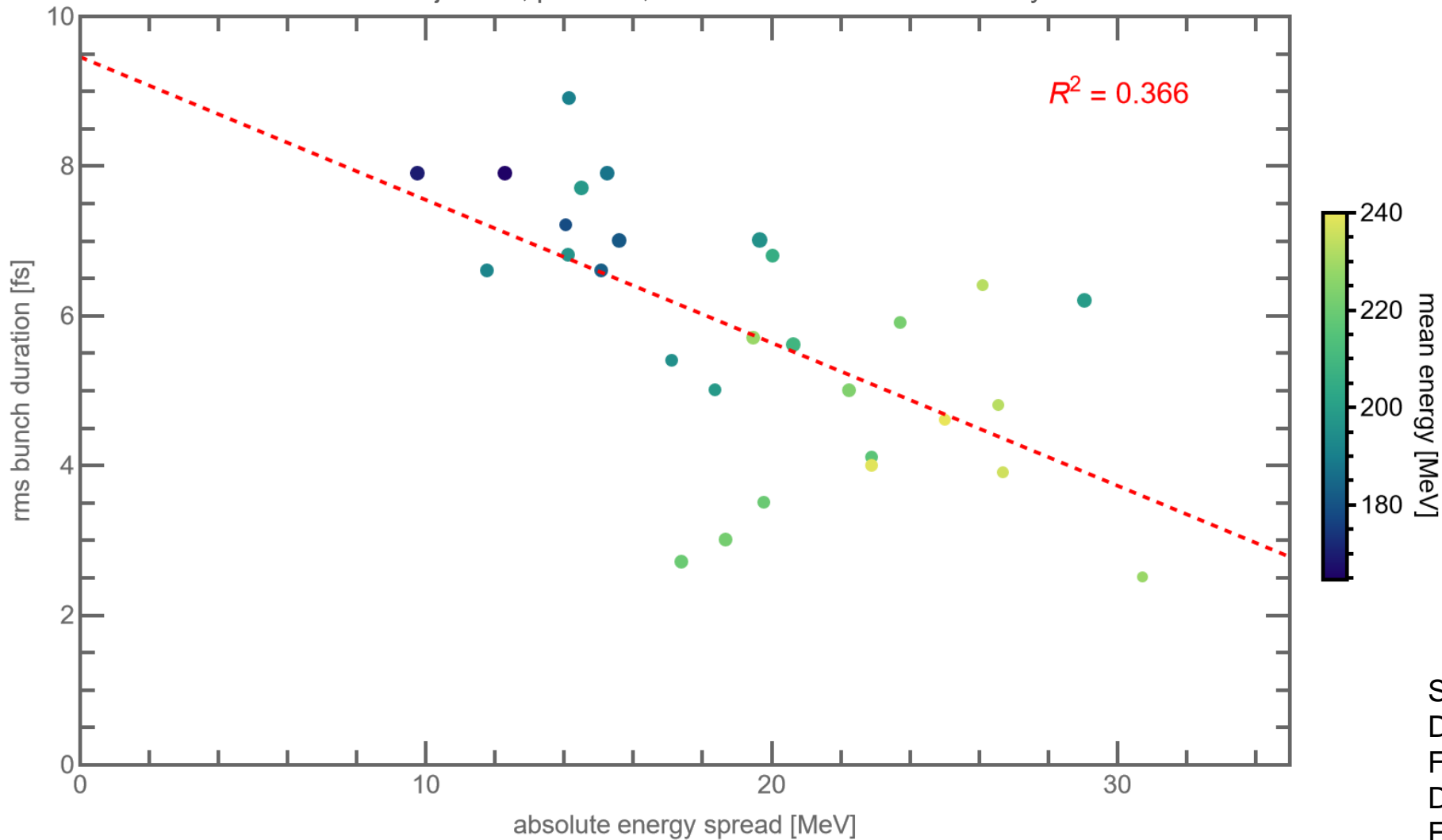
Shock injection, pure He, $3.4 \cdot 10^{18} \text{ cm}^{-3}$ electron density



Dot-areas are proportional to bunch charge.

Correlations in shock injection: Bunch duration vs. absolute energy spread

Shock injection, pure He, $3.4 \cdot 10^{18} \text{ cm}^{-3}$ electron density



Other observed correlations

Higher energies correlate with less charge and higher envelope currents.

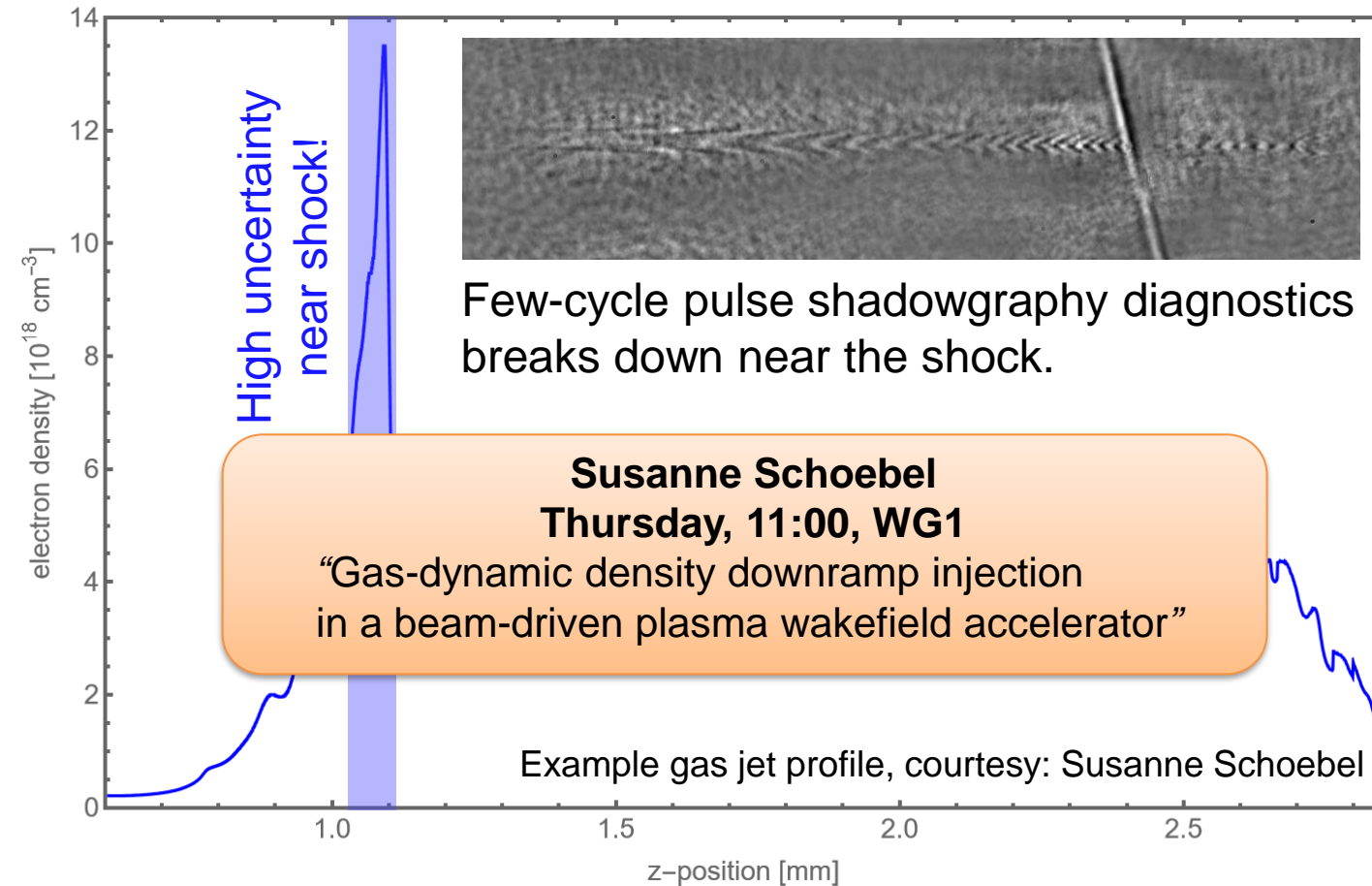
No significant correlation with divergence.

When assuming shot-to-shot variations in shock density contrast, **observed correlations qualitatively agree predictions from PIC simulations.**

- S. Samant et al., PPCF 56, 095003 (2014)
DOI: 10.1088/0741-3335/56/9/095003
- F. Massimo et al., PPCF 59, 085004 (2017)
DOI: 10.1088/1361-6587/aa717d
- F. Massimo et al., PPCF 60, 034005 (2018)
DOI: 10.1088/1361-6587/aaa336

Dot-areas are proportional to bunch charge.

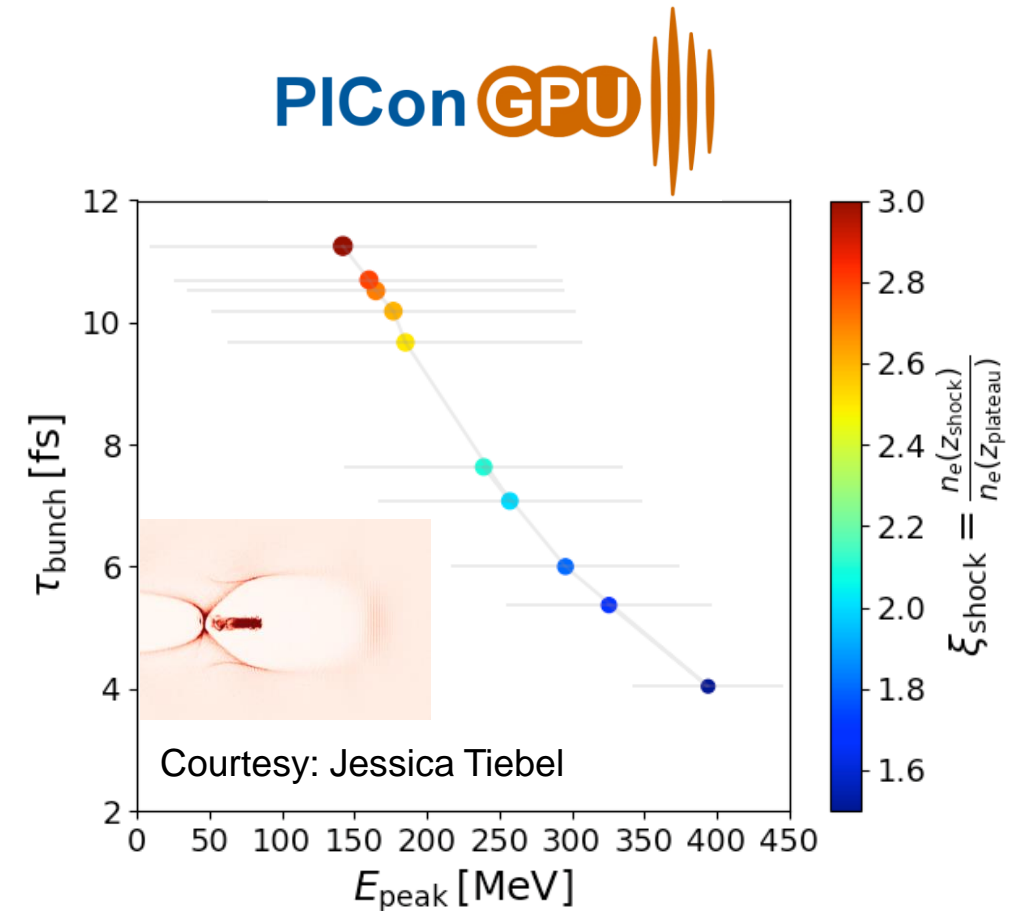
Preliminary analysis: Use bunch duration to deduce shock density contrast



Bunch length is predominantly determined by **shock density contrast** and **beam loading**.

$$L_{\text{bunch}} = C_1 \Delta\lambda_p + C_2 Q^2$$

H. Ekerfelt, et al., Sci. Rep. 7:12229 (2017), DOI: 10.1038/s41598-017-12560-8



Preliminary PIC simulations qualitatively reproduce observed bunch duration to bunch energy correlation.

Further analysis needed.

Conclusions

- Single-shot, ultrabroadband CTR spectroscopy applied for characterizing fs-scale electron beams and its micro-structures for shock injection, self-truncated ionization injection and self-injection in ~800 shots.
- Microbunching structures (~10% form factor) are found to be dominantly characterized by the laser wavelength and its harmonics.
- Correlations in shot-to-shot variations between electron beam durations and current with electron energy, energy spread and charge provide a new window to access the injection dynamics.

Maxwell LaBerge

Wednesday, 11:00, Plenary

“3D structure of microbunched plasma-wakefield-accelerated electron beams inferred by coherent optical transition radiation”





Thank you for your attention!

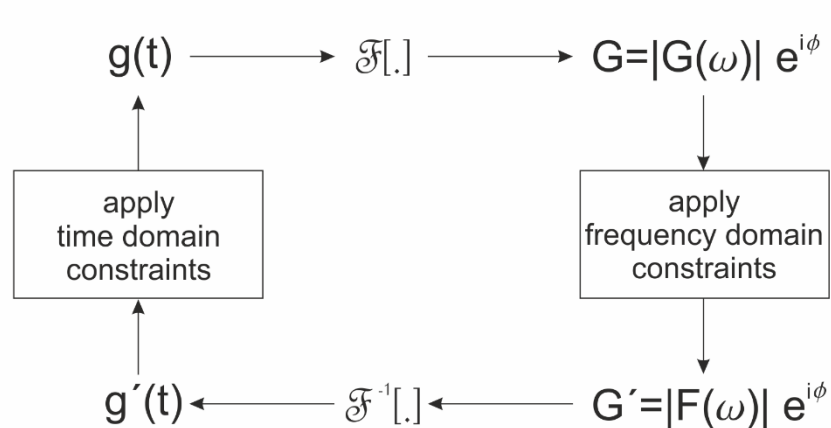
Supplementary material

Retrieve the phase of the form factor

Approximation of CTR form factor

$$F(\omega, \theta) = \int d\vec{r} \rho(\vec{r}) e^{-i\vec{k} \cdot \vec{r}}$$

relates the normalized electron density ρ to a Fourier transform



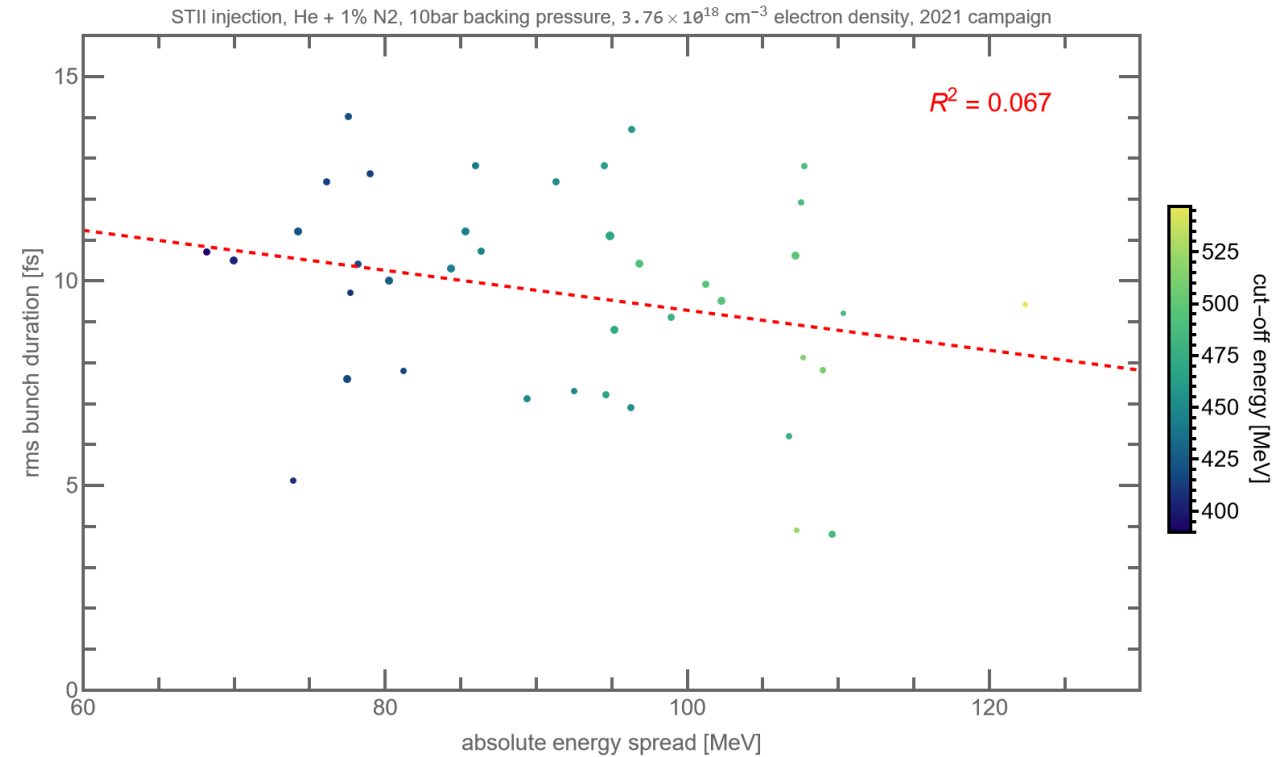
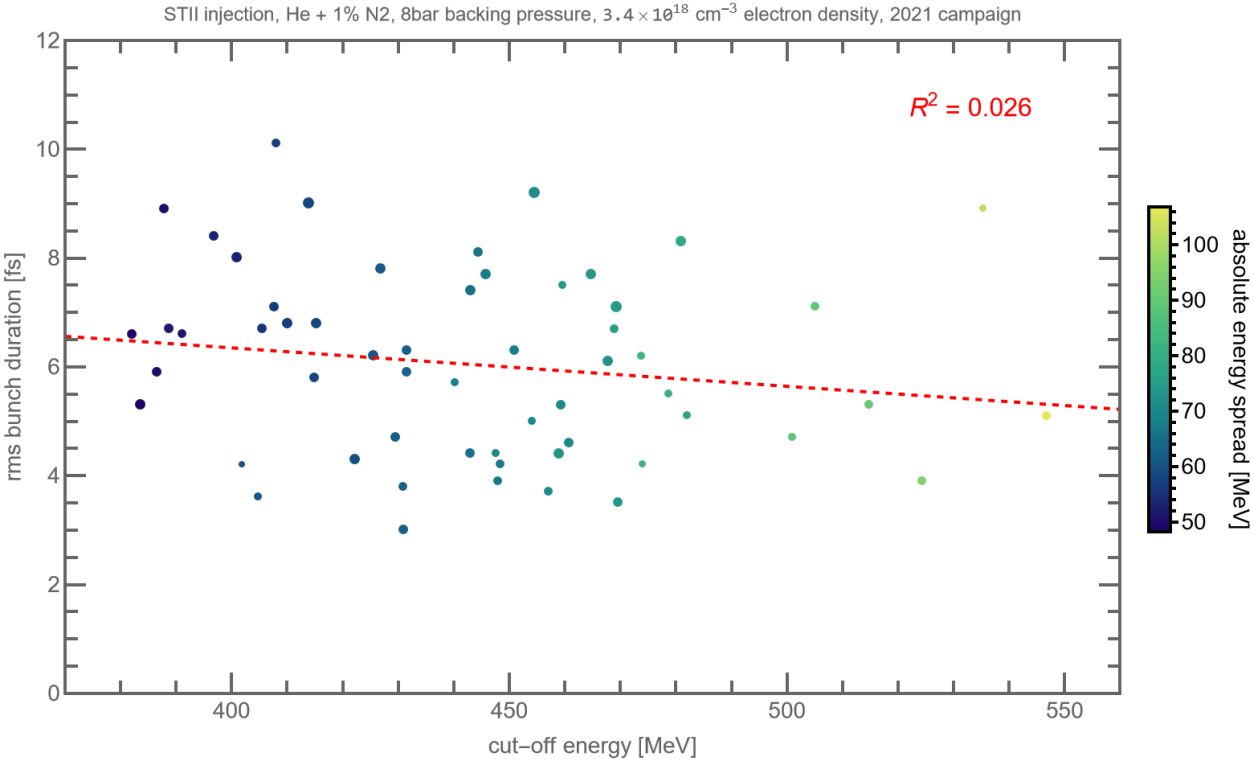
Limitations of direct phase-retrieval methods for CTR spectroscopy without additional data and constraints

Schmidt et.al., arXiv:1803.00608 (2018)

Algorithms used to solve the inverse problem

- Bubblewrap algorithm
Bajlekov, et.al., PRSTAB 16, 040701(2013)
Heigoldt, et.al., PRSTAB 18, 121302(2015)
- Correlate reconstruction candidates according to ambiguities from translation and inversion symmetry
Pelliccia, et.al., Opt. Lett. 37, 262-264 (2012)
Pelliccia and Sen, NIMA 764, 206-214 (2014)
- Apply zero-frequency constraints, i.e. total charge constraint from electron spectrometer data
- Complementary method: Kramers-Kronig for some initial estimates
Lai and Sievers, NIMA 397, 221-231 (1997)

STII injection at $n_{eI} = 3.4 \cdot 10^{18} \text{ cm}^{-3}$



Dot-areas are proportional to bunch charge.